



**HAL**  
open science

## GPS/Galileo RAIM performance in presence of multiple pseudorange failures due to interference

Anaïs Martineau, Christophe Macabiau, Olivier Julien, Igor V. Nikiforov,  
Benoit Roturier

► **To cite this version:**

Anaïs Martineau, Christophe Macabiau, Olivier Julien, Igor V. Nikiforov, Benoit Roturier. GPS/Galileo RAIM performance in presence of multiple pseudorange failures due to interference. ION GNSS 2007, 20th International Technical Meeting of the Satellite Division of The Institute of Navigation, Sep 2007, Fort Worth, United States. pp 3045 - 3056. hal-01022130

**HAL Id: hal-01022130**

**<https://enac.hal.science/hal-01022130v1>**

Submitted on 20 Nov 2014

**HAL** is a multi-disciplinary open access archive for the deposit and dissemination of scientific research documents, whether they are published or not. The documents may come from teaching and research institutions in France or abroad, or from public or private research centers.

L'archive ouverte pluridisciplinaire **HAL**, est destinée au dépôt et à la diffusion de documents scientifiques de niveau recherche, publiés ou non, émanant des établissements d'enseignement et de recherche français ou étrangers, des laboratoires publics ou privés.

# GPS/Galileo RAIM Performance in Presence of Multiple Pseudorange Failures due to Interference

Anais Martineau, *ENAC*  
Christophe Macabiau, *ENAC*  
Olivier Julien, *ENAC*  
Igor Nikiforov, *UTT*  
Benoît Roturier, *DTI*

## BIOGRAPHY

Anais Martineau graduated in July 2005 as an electronics engineer from the Ecole Nationale de l'Aviation Civile (ENAC) in Toulouse, France. She is now working as a Ph.D. student at the signal processing lab of the ENAC where she carries out research on integrity monitoring techniques.

Christophe Macabiau graduated as an electronics engineer in 1992 from the ENAC in Toulouse, France. Since 1994, he has been working on the application of satellite navigation techniques to civil aviation. He received his Ph.D. in 1997 and has been in charge of the signal processing lab of the ENAC since 2000. His research now also applies to vehicular, pedestrian and space applications, and includes advanced GNSS signal processing techniques for acquisition, tracking, interference and multipath mitigation, GNSS integrity, as well as integrated GNSS inertial systems and indoor GNSS techniques.

Olivier Julien is an assistant professor at the Signal Processing lab of ENAC. His research interests are GNSS receiver design, GNSS multipath and interference mitigation techniques, and GNSS interoperability. He graduated as an electronics engineer in 2001 from the ENAC and received his PhD in 2005 from the Department of Geomatics Engineering of the University of Calgary, Canada. He is the recipient of the 2006 Bradford W. Parkinson award.

Igor Nikiforov received his M.S. degree in automatic control from the Moscow Physical-Technical Institute in 1974, and the Ph.D. in automatic control from the Institute of Control Sciences (Russian Academy of Science), Moscow, in 1981. He joined the University of

Technology of Troyes (UTT) in 1995, where he is Professor and Head of the Institute of Computer Sciences and Engineering of Troyes. His scientific interests include statistical decision theory, fault detection/ isolation/ reconfiguration, signal processing and navigation.

Benoît Roturier graduated in Engineering from the ENAC in 1985 and obtained a PhD diploma in Electronics from Institut National Polytechnique of Toulouse in 1995. His activities are within the France aviation administration (DGAC) since 1987, where he has been successively managing installation of Instrument Landing Systems (ILS) at STNA, head of the research laboratory on CNS systems of ENAC, head of satellite navigation subdivision (GNSS) within DSNA/DTI (Direction des Services de la Navigation Aérienne/Direction de la Technique et de l'Innovation). Since 2007, he is the project manager of satellite navigation (GNSS) and area navigation (RNAV) implementation for DSNA/DTI.

## ABSTRACT

In a multi constellation context, demanding phases of flight such as APV operations can be targeted using Receiver Autonomous Integrity Monitoring (RAIM) to check GNSS integrity. This is why it is necessary to characterize all failure modes inducing range errors of the order of a few meters. One of these failure modes is radio frequency interference which causes very penalizing errors since they can affect several measurements at the same time.

This work focuses on advanced and classical GPS/Galileo RAIM performance degradation evaluation in presence of multiple failures due to interference when stringent phases of flight are targeted.

The way the User Equivalent Range Error UERE, especially the receiver noise residual error, is computed is first reminded in this paper. The main unintentional interference sources to be accounted for in the ARNS are then given and their impact is discussed. More particularly an expression of the code tracking error envelope in presence of CW interference is proposed. A complete pseudo range measurements model is given taking into account the interference effect.

The issue of integrity monitoring in presence of interference is studied considering two different algorithms: the Sequential Constrained Generalized Likelihood Ratio Test based RAIM and the Snapshot Least Squares Residuals RAIM.

The last part of this paper is dedicated to GPS/Galileo RAIM simulations that have been conducted using this proposed model on GPS L1/L5 and Galileo E1/E5b pseudorange measurements under different conditions: nominal ones, with a CW interference with a power within the GPS L1 C/A interference mask or 20dB above this mask. CW were added on two frequencies: the worst Galileo spectrum line and the worst GPS spectrum line. The two integrity monitoring algorithms formerly described have been tested for two modes of flight APV 1 and APV2. The goal of these simulations is not to detect interference, it is to observe RAIM capacity to detect a bias, corresponding to a satellite failure with a probability of occurrence of  $10^{-4}/h$ , in presence of interference

It is seen that there is no impact of CW interference within the interference mask. Both algorithms studied manage to detect dangerous biases with the required probability and their actual performance are not degraded. On the contrary, CW interference with a power 20 dB above the mask has an important effect on pseudo range error variance and can even lead to misleading situation using classical snapshot RAIM. However, in any case, if advanced methods of monitoring integrity are used that is to say measuring the ability of detecting dangerous biases, the user will be protected from hazardous misleading situation.

## INTRODUCTION

Receiver Autonomous Integrity Monitoring (RAIM) is a simple and efficient solution to check the integrity of GNSS in civil aviation applications such as Non Precision Approach. In a multi constellation context, implying a large number of satellite and new signals, and thanks to advanced algorithms, more demanding phases of flight such as APV operations can be targeted. Given the stringent requirements of potential applications in the future, it seems necessary to characterize all failure modes inducing range errors of the order of a few meters. Indeed, for these applications, these defaults can more than ever

lead to a degradation of the navigation solution and thus to an integrity risk situation.

One of these failure modes is radio frequency interference which causes very penalizing errors since they can affect several measurements at the same time. The main effect of interference is to degrade the signal to noise ratio and that can make classical integrity monitoring methods ineffective since they are based on a noise level assumption. This level corresponds to the RFI mask adopted to define the RF environment for which the receiver must have a compliant performance. But in any case, even with large power interference above the mask or in presence of very narrow band interference, the integrity performance of the receiver must be compliant with the specifications. This is why it is useful to analyse the performance of existing algorithms in such constraining environments and especially their ability to detect a bias on a pseudo range corresponding to a satellite failure with a probability of occurrence of  $10^{-4}/h$  that will lead to a positioning failure.

Sequential RAIM based on the constrained Generalized Likelihood Ratio (GLR) test, which is based on a formalized definition of a horizontal or vertical error that must be considered as a positioning failure, theoretically constitutes a very competitive technique and will be tested. The classical snapshot LSR RAIM performance will also be studied.

This work focuses on GPS/Galileo RAIM performance degradation evaluation in presence of multiple failures due to interferences when stringent phases of flight such as APV operations are targeted.

The paper is organized as follows. First, classical User Equivalent Range Error variance model will be recalled. Then an analysis of the impact of different kinds of interferences on pseudo range measurements will be conducted in order to propose a complete model of smoothed pseudo range. Integrity monitoring issue in presence of interference will be formulated and finally RAIM simulations results will be presented.

## I – PSEUDO RANGE ERROR BUDGET

The goal of this section is to compute pseudo range measurement error variance model in nominal conditions that is to say in presence of noise or in presence of interference that can be assimilated to noise.

These pseudo range measurement error variances are gathered in the User Equivalent Range Error UERE variance and will constitute a major input of RAIM availability computation. This is why the following contributions are to be considered: orbit determination and synchronisation error, troposphere residual error, ionosphere residual error, multipath residual error and

receiver noise residual error. This last contribution is detailed in the following section.

### I-1 Receiver noise residual error

#### Computation of error variance of a code-tracking loop

The error variance of the code-tracking loop will depend on the choice of the discriminator. Assuming that interference can be assimilated to white noise and for Early Minus Late Power discriminator (for example):

$$\sigma_{EMLP}^2 = \frac{B_L(1 - 0.5B_L T) \int_{-B/2}^{B/2} G(f) \sin^2(\pi f C_s) df}{\frac{C}{N_0} \left( 2\pi \int_{-B/2}^{B/2} f G(f) \sin(\pi f C_s) df \right)^2} \times \left( 1 + \frac{\int_{-B/2}^{B/2} G(f) \cos^2(\pi f C_s) df}{\frac{C}{N_0} T \left( \int_{-B/2}^{B/2} G(f) \cos(\pi f C_s) df \right)^2} \right), \text{ where}$$

$B_L$  (Hz) the one sided bandwidth of the equivalent loop filter

$T$  the data period,  $T = 1/f_D$

$G$  the power spectrum density of the signal

$C/N_0$  the signal to noise ratio

$C_s$  the chip spacing

$B$  the two sided bandwidth of the front end filter

Without considering the temporal repetition period of the PN sequence, the power spectrum density expression of the BPSK signal is:

$$G(f) = T_c \left( \frac{\sin \pi f T_c}{\pi f T_c} \right)^2$$

with  $T_c$  the code period.

This expression is used for GPS L1, GPS L5 and GALILEO E5b code tracking loop error variance. For Galileo E1, the normalized power spectrum density of the BOC(1,1) is equal to:

$$G(f) = T_c \left( \frac{1 - \cos(\pi f T_c)}{\pi f T_c} \right)^2$$

The error variance of the code tracking loop, error due to noise, can be thus computed for different kind of signals.

#### Iono free measurements

In nominal mode, the pseudorange measurements that are available to the aircraft receiver are the GPS L1, GPS L5, GALILEO E1, GALILEO E5a, GALILEO E5b code and phase measurements. But for future civil aviation GNSS

receivers complying with EUROCAE requirements, dual frequency measurements will be combined into a single composite measurement called the iono-free measurement, corrected for ionospheric error.

Therefore, from GPS L1 – L5, and from GALILEO E1 – E5b, two distinct iono-free measurements are built.

Denoting  $m(k)$  the measurement at the instant  $k$  (representing  $P(k)$  the code measurement or  $\varphi(k)$  the phase measurement):

$$m_{1-5}(k) = \frac{f_1^2}{f_1^2 - f_5^2} m_1(k) + \frac{f_5^2}{f_5^2 - f_1^2} m_5(k)$$

$$\text{and } \frac{f_{L1}^2}{f_{L1}^2 - f_{L5}^2} \approx 2.261, \quad \frac{f_{L5}^2}{f_{L5}^2 - f_{L1}^2} \approx -1.261,$$

$$\frac{f_{E1}^2}{f_{E1}^2 - f_{E5b}^2} \approx 2.422 \quad \text{and} \quad \frac{f_{E5b}^2}{f_{E5b}^2 - f_{E1}^2} \approx -1.422$$

No significant correlation factor can be expected for the noise and multipath error affecting the different measurements made on the four carrier frequencies. This is why the standard deviation of the error affecting the iono-free measurement is modelled as:

$$\sigma_{L1-L5} = \sqrt{2.261^2 \sigma_{L1}^2 + 1.261^2 \sigma_{L5}^2}$$

$$\sigma_{E1-E5b} = \sqrt{2.422^2 \sigma_{E1}^2 + 1.422^2 \sigma_{E5b}^2}$$

#### Smoothing

Once elaborated, these two GPS and GALILEO iono-free measurements are then smoothed to reduce the influence of noise and multipath [9]:

$$\sigma_{\bar{p}}^2 \approx \frac{\sigma_p^2}{2T_{smooth}}$$

where  $T_{smooth}$  is the time smoothing constant in seconds

$\sigma_p^2$  is the raw code pseudorange measurement error variance

$\sigma_{\bar{p}}^2$  is the smoothed code pseudorange measurement error variance

Finally, the receiver noise residual error variance  $\sigma_{noise}^2$  is obtained. It corresponds to the receiver noise, thermal noise, inter channel bias and processing error.

#### I-2 Multipath error

The smoothed multipath error for the airborne equipment is described by  $\sigma_{multipath} = 0.3 + 0.53 \cdot \exp\left(-\frac{\theta}{10 \text{ deg}}\right)$

where  $\theta$  is the elevation angle in degree of the considered satellite. This was validated and adopted for GPS L1 C/A. It is also assumed here for GPS L5, Galileo E1 and E5b although smaller error can be anticipated [6].

### I-3 Ionospheric residual error

In the case of a dual frequency receiver with ionospheric correction the ionospheric residual error is not considered as significant,  $\sigma_{iono} = 0$ .

### I-4 Tropospheric residual error

The model for the residual error for the tropospheric delay estimate is:  $\sigma_{tropo} = 0.12m(El)$  where  $El$  is the elevation angle and the tropospheric correction mapping function  $m(El) = \frac{1.001}{\sqrt{0.002001 + \sin^2(El)}}$ .

This model was adopted for GPS L1 C/A and is assumed for GPS L5 and Galileo E1 and E5b.

### I-5 User equivalent range error

The User Equivalent Range Error is the value reflecting the error budget and it is based on the computation of the following contributions: orbit determination and synchronisation error, troposphere residual error, ionosphere residual error, multipath residual error and receiver noise residual error.

$$\sigma_{UERE}^2 = \sigma_{URA}^2 + \sigma_{iono}^2 + \sigma_{air}^2 + \sigma_{tropo}^2 + \sigma_{L1/E5bias}^2$$

$$\text{with } \sigma_{air}^2 = \sigma_{noise}^2 + \sigma_{multipath}^2$$

It is supposed that  $\sigma_{URA} = 0.65$  m and  $\sigma_{L1/E5bias} = 0$ .

The figure 1 represents the obtained Galileo smoothed iono free UERE for different elevation angle and for different C/N0 on E1. It can be seen that the signal to noise ratio has to be very low to have a significant effect on the global UERE.

## II – INTERFERENCE EFFECTS ON PSEUDO RANGE MEASUREMENT

The main interference sources to be accounted for in the ARNS are, for unintentional interferences:

- CW interferences on all bands
- Wideband interferences on all bands
- Pulsed Interferences (DME/TACAN on L5, Radars on E5b, UWB)

This paper only focuses on interference on L1 and thus pulsed interferences are not considered.

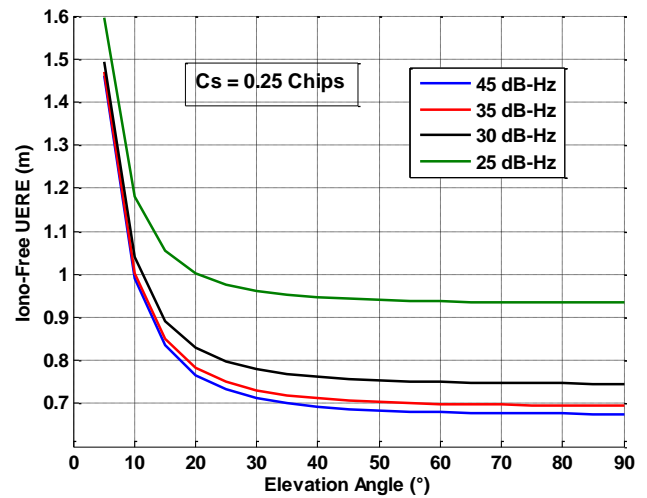


Fig 1 - Galileo smoothed iono-free UERE for C/N0=45 dB-Hz on E5b and different C/N0 on E1

### II-1 Wideband interferences

Wideband interferences are commonly supposed to be white noise with limited bandwidth. The code tracking error variance for large and narrow band interference is given in [5]:

$$\sigma_{EMLP}^2 = B_L (1 - 0.5 B_L T) \left( \frac{\int_{-B/2}^{B/2} G(f) G_w(f) \sin^2(\pi f C_s) df}{C \left( \int_{-B/2}^{B/2} f G(f) \sin(\pi f C_s) df \right)^2} + \frac{\left( \int_{-B/2}^{B/2} G(f) G_w(f) df \right)^2 - \left| \int_{-B/2}^{B/2} G(f) G_w(f) e^{i2\pi f C_s} df \right|^2}{C^2 T \left( \int_{-B/2}^{B/2} f G(f) \sin(\pi f C_s) df \right) \int_{-B/2}^{B/2} G(f) \cos(\pi f C_s) df} \right)$$

where  $B_L$  (Hz) is the one sided bandwidth of the equivalent loop filter

- $T$  is the data period,  $T = \frac{1}{f_D}$
- $G$  is the power spectrum density of the signal
- $C/N_0$  is the signal to noise ratio
- $C_s$  is the chip spacing
- $B$  is the two sided bandwidth of the front end filter
- $G_w$  is the power spectrum density of the interference

## II-2 CW interferences

A Carrier Wave interference is a sinusoidal waveform that can be continuous or pulsed. If this narrowband interference has a high power it can be disastrous for the receiver, especially if it is centred in the GNSS frequency band.

The general model of a CW interference is given by:

$$J = A_j \cos(2\pi(f_i + \Delta f_j)t - \theta_j)$$

where

$A_j$  is the amplitude of the CW,

$\Delta f_j$  is the frequency offset of the jammer with respect to the considered GNSS signal's carrier frequency,

$\theta_j$  is the phase of the jammer.

$f_i + \Delta f_j$  is the central frequency

The power spectrum density of the noise and the interference will be:

$$G_w(f) = \frac{N_0}{2} + \frac{A_j^2}{4} \delta(f - (f_i + \Delta f_j))$$

As it has been seen several models were already proposed to analyse the effect of interference on GNSS signal processing. Most of them model the effect of interference at correlator output as the effect of equivalent additional white noise at the receiver input.

However, as pointed out by many authors, the tracking error induced by the presence of interference can not be always be modelled as the tracking error induced by an equivalent increased white noise. A distinction must be made depending on the bandwidth of the incoming interference. In fact these models are valid as long as the bandwidth of the interference is quite large compared to the inverse duration of the integration. Thus it is desired to complete these models for narrowband interference and in particular for the case where the receiver is affected by CW interference.

By analyzing the correlator output components, an expression of the code tracking error envelope in presence of CW interference is proposed [3]:

$$M = \left| \frac{A_j}{\alpha A} C_c(k_0) \frac{\sin(\pi \delta f T_D)}{\pi \delta f T_D} \sin(\pi k_0 f_R C_s) \right|$$

where

-  $M$  is the absolute value of the maximum code tracking error induced by the CW in chip

-  $C_s$  is the Early-Late chip spacing in seconds

-  $\frac{A_j}{A}$  is the relative amplitude of the CW compared to the useful GNSS signal

-  $C_c(k_0)$  is the relative amplitude of the PRN code ray which is the closest to the interference

-  $\delta f$ , the difference between the CW frequency and the closest signal peak

-  $\alpha$  is the slope of the spreading waveform autocorrelation function in  $\frac{C_s}{2}$ .

The code tracking error oscillates within this envelope.

Assuming that the code tracking error is uniformly distributed on  $[-M, M]$ , its variance will be  $\sigma^2 = \frac{M^2}{3}$ . Assuming that the code tracking error can be written  $\varepsilon = M \sin(\theta)$  with  $\theta$  uniformly distributed on  $[0, 2\pi]$ , its variance will be  $\sigma^2 = \frac{M^2}{2}$ . This last assumption is more realistic and is chosen.

To predict this error variance, the Doppler shift has to be computed for each satellite-user couple in order to precisely know the difference between the CW frequency and the closest signal peak of the considered PRN.

By this way the receiver error component due to CW interference is obtained and is to be added to the one due to noise obtained by usual formula.

## III MODEL PROPOSITION

In this part we intend to give a complete model of pseudo range measurements, including interference effects.

When some interfering signal is superimposed to the received useful signal, this can have the following three impacts on the pseudo range measurements:

- the measurements are affected by some additional noise

- one or several measurements are affected by a bias (divergence of measurement)

- some or all of the measurements are no longer available (loss of tracking)

An RFI mask was adopted to define the RF environment for which the receiver must have compliant performance, but in any case, even with large power interference above the mask, the integrity performance of the receiver must be compliant with the specifications. This is why it is needed to take into account every interference effect in this model that will feed RAIM algorithms.

This model has also to consider the potential case where several pseudo range measurement are simultaneously affected by errors from different sources that can be a clock satellite failure or an interference effect.

The proposed model of smoothed pseudorange measurement is:

$$Y(k) = h(X(k)) + E(k) + B(k) + D(k)$$

where

- $E(k)$  error measurement that gathers the ionosphere, the troposphere, the ephemeris, the clock errors (with a correlation time of one hour) and the multipath (with a correlation time corresponding to the receiver smoothing time):

$$E(k) = \text{iono}(k) + \text{tropo}(k) + \text{URA}(k) + \text{multipath}(k)$$

- $B(k)$  smoothed measurement error due to the noise that includes interference effects. Its correlation time corresponds to the receiver smoothing time. In the absence of interference, the standard deviation of the corresponding unsmoothed error will be taken as in section I. In presence of wideband or narrowband interference, the standard deviation of the corresponding unsmoothed error will be taken as in section II-1. In presence of CW interference, the corresponding unsmoothed error will be taken as a random variable with envelope as expressed in II-2.

- $D(k)$  additional error measurement due to the tracking of mixed useful signal and interference:  $D(k)$  is supposed to be a combined step ramp error, in order to model an error with a slow erratic behaviour.

### Loss of tracking

A criterion allowing predicting the loss of lock of a GNSS signal disturbed by a CW interference is needed. Several tests have been conducted and it has seemed relevant to set the loss of lock threshold on the envelope value. When the envelope value reaches  $M = 40$  m the corresponding satellite signal is considered as not tracked anymore.

## IV – INTEGRITY MONITORING IN PRESENCE OF INTERFERENCE

The effect of interference on integrity monitoring function will depend on the RAIM algorithm that is used.

According to [2], the detection function of a RAIM FDE algorithm is defined to be available when the constellation of satellites provides a geometry for which the missed alert and false alert requirement can be met on all satellites being used for the applicable alert limit and time to alert. Corresponding civil aviation requirements for

different modes of flight are represented by those typical values:

Mode of flight	HAL / VAL	Integrity risk	Time to alert
Terminal	1 NM	$10^{-7} / h$	15 s
NPA	0.3 NM	$10^{-7} / h$	10 s
APV I	40m/50m	$2 \times 10^{-7} / 150$ s	10 s
APV II	40m/20m	$2 \times 10^{-7} / 150$ s	6 s

### IV -2 Sequential constrained GLR RAIM algorithm

Sequential GLR RAIM algorithm availability is characterized by its capacity to detect every critical bias on each pseudorange measurement with a detection rate compliant with the Pmd, within the time to alert. For each pseudo range the critical bias is the smallest additional error that will lead to a positioning failure, that is to say  $Horizontal\ Error > HAL$  or  $Vertical\ Error > VAL$  with a probability equal to the integrity risk. The implementation of such a RAIM needs to compute for each satellite channel these smallest biases which correspond to the worst case detection/exclusion situations.

The way each critical bias is computed is recalled in appendix.

The amplitude of this minimal bias will depend on the assumed level of noise. In presence of interference, affected PRN suffer from pseudo range measurement error variance augmentation. Therefore the corresponding critical biases are smaller than usual and thus more difficult to detect.

In presence of interference different performances can be computed:

- the actual performance: biases that are to be detected take into account the actual level of noise (the interference effect)
- the assumed performance: the one that it is given to the user, biases that are to be detected only take into account an assumed nominal level of noise

### IV- 3 Snapshot LSR RAIM algorithm

Snapshot LSR RAIM algorithm is the classical RAIM. It works differently than the advanced RAIM that has been described in the previous subsection. Here the availability of detection or exclusion function is obtained by computing Horizontal and Vertical Protection Level and comparing them to Horizontal and Vertical Alert Limit.

These protection levels depend on the assumed level of noise. Therefore the corresponding availability depends on the assumed level of noise.

In presence of interference, several parameters can be computed:

- the assumed protection levels: given to the user are the ones that correspond to nominal conditions since the RAIM made an assumption on the value of the pseudorange variance errors and does not estimate them
- the actual protection levels are the ones that takes into account the real impact of interference on pseudorange error variance
- the probability of detection of every critical bias on each pseudo range (biases computed taking into account the impact of interference)

These parameters correspond to different availability figures:

- the assumed availability, obtained by comparing the assumed xPL to the xAL
- the actual availability, obtained by comparing the actual xPL to the xAL
- the availability for critical biases detection, obtained by comparing the probability of detection of every critical bias to 1- Pmd

## V – RAIM SIMULATIONS

### V -1 Assumptions

For all simulations that have been conducted through this study an optimal 27-Galileo constellation and an optimal 24-GPS constellation have been used and the measurements that have been supposed to be available were GPS L1/L5 and Galileo E1/E5b.

Two integrity monitoring algorithms have been tested: the Sequential Constrained Generalized Likelihood Ratio Test based RAIM and the Snapshot Least Squares Residuals RAIM, for two modes of flight APV 1 and APV2.

Simulations have been conducted for one user position in Toulouse (France) located N 43.56°, E 1.48°, ALT 201.61 meters. A 5° mask angle has been used for GPS and a 10° mask angle for Galileo

CW interference have been injected on two frequencies: the worst Galileo spectrum line  $f_j = 839kHz$  and the worst GPS spectrum line  $f_j = 227kHz$ . The interference mask that it is referred to is the GPS L1 C/A interference mask corresponding to a power of -156.5 dBW.

### IV -2 UERE standard deviation variation

Several RAIM simulations have been conducted using the complete model of pseudo range presented in the last section.

One of the aspects of this new model is a possible augmentation of error amplitude on pseudorange

measurement especially in presence of CW interference. To evaluate this impact, the variation of variance pseudorange error has been observed through 24 hours simulations. For each epoch, the minimum, the maximum and the average UERE standard deviation have been computed across the available PRN.

For CW simulations it is to be noticed that PRN with a code tracking error envelope value superior to the loss lock threshold have been removed from the computation.

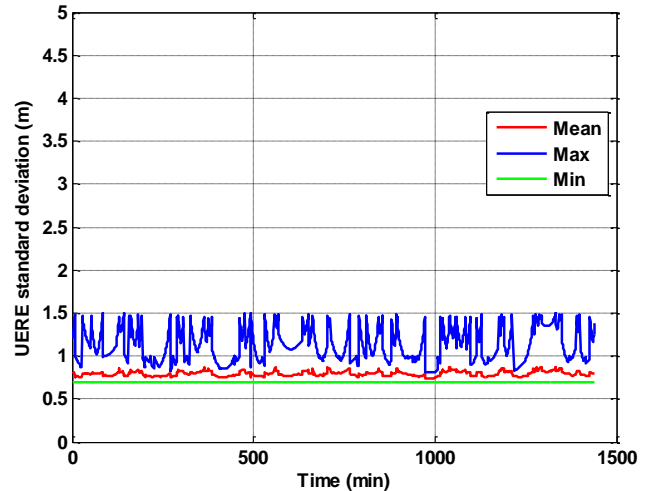


Fig. 2 - Reference simulation

As it can be seen on figures 2 and 3, that a CW within the interference mask will lead to UERE standard deviation with nearly the same mean as the ones obtained through reference simulations. Nevertheless UERE standard deviation can reach 2 m instead of 1.5 m.

A more powerful interference (20 dB above the mask) will have a more significant impact on the maximum value of UERE standard deviation that can be reached (up to 4.5m) and lead to a 0.5 m augmentation of the mean (figure 4).

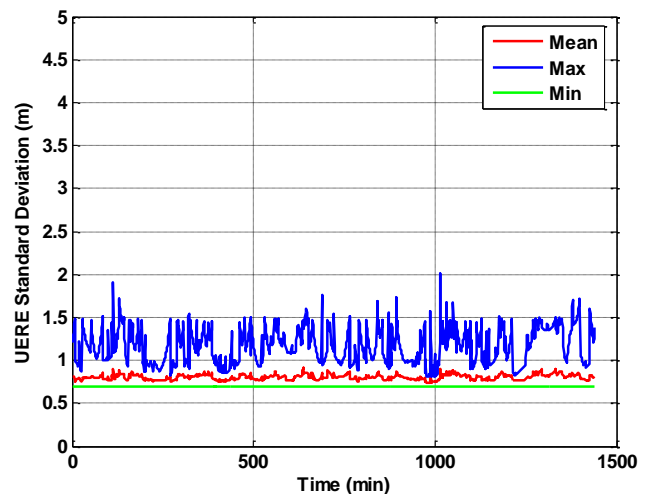


Fig 3 - CW -156.5dBW on the worst Galileo spectrum line



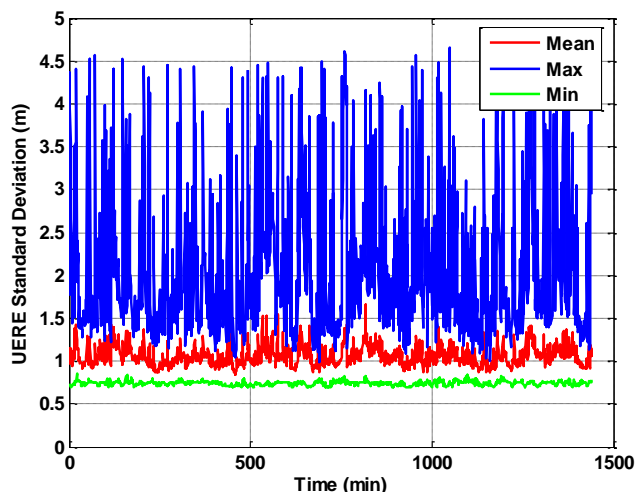


Fig 4 - CW -135.5dBW on the worst Galileo spectrum line

#### IV -2 Sequential constrained GLR RAIM algorithm

Different results are presented for each simulation conducted:

- the average detection rate (detection of critical biases corresponding to each pseudo range)
- the percentage of time when the detection function is available (for a given moment this function is considered as available if the detection rate copes with the Pmd).

Table 1 presents the actual performance and table 2 resumes the assumed one, that is to say the performance given to the user.

Conditions	Mode of flight	Detection function Availability	Average detection rate
Nominal Noise	APV1	0.999	0.998
	APV2	0.999	0.998
CW worst GPS line -156.5dBW	APV2	0.999	0.998
CW worst GPS line -135.5dBW	APV2	0.988	0.997
CW worst Galileo line -135.5dBW	APV2	0.994	0.998
CW worst Galileo line -156.5dBW	APV2	0.999	0.998

Table 1- Sequential constrained GLR actual availability

As it can be seen on figure 5, even if the bias to detect with the required probability to consider the RAIM as available is smaller for APV 2, the detection rate is the same for APV 1 and 2. This is due to the great number of visible satellite that makes detection easier.

If a CW interference within the interference mask is injected on GPS worst line, critical biases that lead to a positioning failure are quite the same as the reference

simulation ones. This is why sequential constrained GLR RAIM has the same availability.

Conditions	Mode of flight	Assumed Detection function availability	Average assumed detection rate
CW worst GPS line -156.5dBW	APV2	0.999	0.998
CW worst GPS line -135.5dBW	APV2	0.988	0.997
CW worst Galileo line -135.5dBW	APV2	0.994	0.998
CW worst Galileo line -156.5dBW	APV2	0.999	0.998

Table 2- Sequential constrained GLR assumed availability

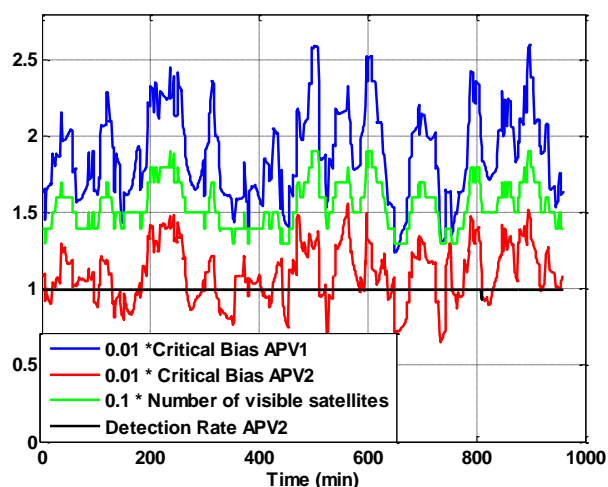


Fig 5 - Sequential Constrained GLR RAIM-APV 1 & 2 Reference Simulations- Nominal Conditions

A CW interference 20 dB above the mask acts differently on sequential constrained GLR RAIM since it visibly degrades its ability to detect critical bias. Three losses of lock can occur if CW is centred on GPS worst line (figures 6, 7) and up to four losses of lock can occur if CW is centred on Galileo worst line (figures 8, 9). Nevertheless, the algorithm does not produce misleading information: if the actual detection function is not available, neither is the assumed detection function.

#### IV- 3 Snapshot LSR RAIM algorithm

Simulations made under nominal conditions have two main aspects:

- Computing the protection levels and comparing them to corresponding alarm limit, table 3
- Injecting critical biases on pseudo range measurement and trying to detect them, table 4

Under nominal conditions the detection function of RAIM LSR for APV 1 operation is always available, whatever the availability evaluation technique.

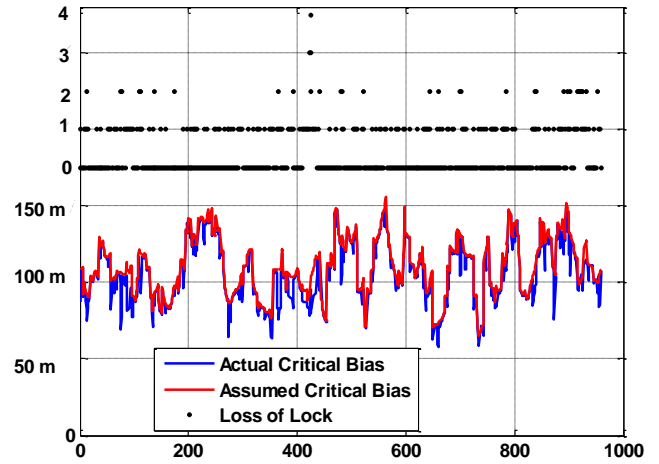
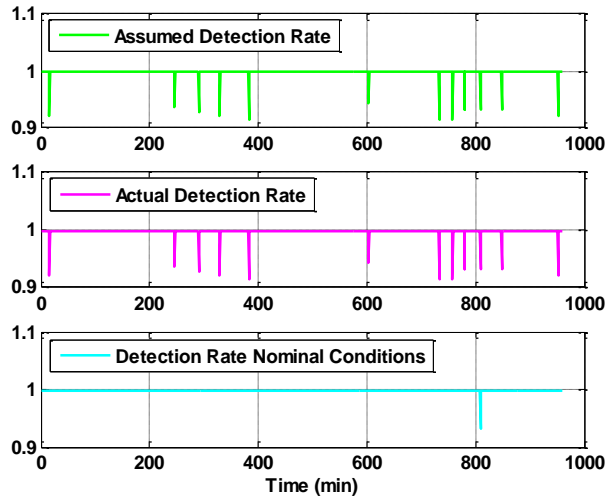


Fig 8 & 9 - Sequential Constrained GLR RAIM - APV2 - CW on worst Galileo P=-135.5dBW

This is not the same for APV 2 operation since actual availability will depend of the way of measuring it. LSR algorithm will be always able to detect every critical bias but actual HPL and VPL are not necessarily lower than HAL and VAL.

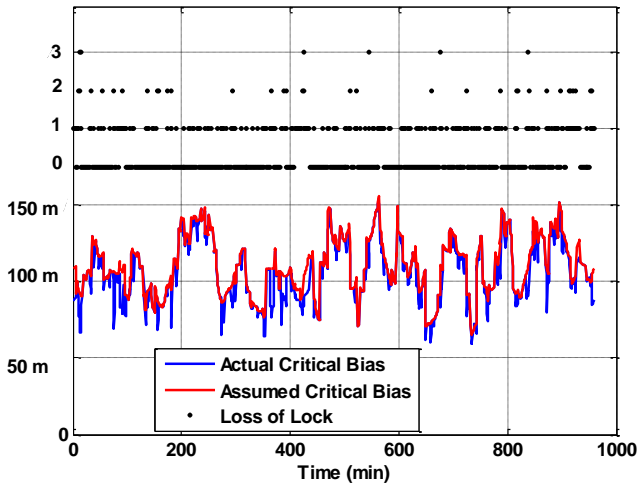
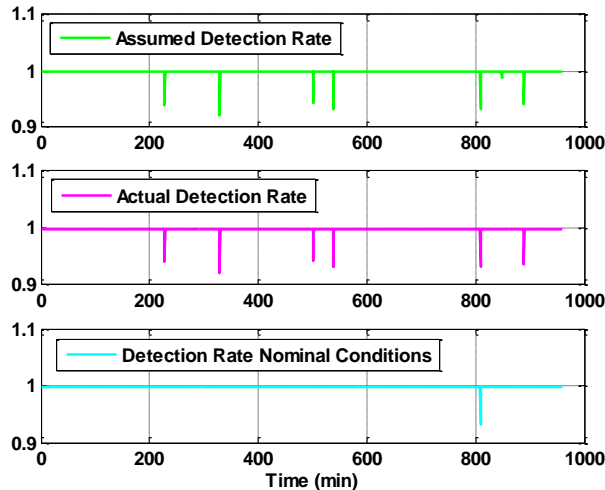


Fig 6 & 7 - Sequential Constrained GLR RAIM - APV2 - CW on worst GPS line P=-135.5dBW



Conditions	Mode of flight	Detection function Availability	Average detection rate
Nominal Noise	APV1	1.00	0.998
	APV2	1.00	0.998
CW worst GPS line -156.5dBW	APV1	1.00	0.998
	APV2	1.00	0.998
CW worst GPS line -135.5dBW	APV1	1.00	0.998
	APV2	0.943	0.992
CW worst Galileo line -156.5dBW	APV1	1.00	0.998
	APV2	1.00	0.998
CW worst Galileo line -135.5dBW	APV1	1.00	0.998
	APV2	0.956	0.993

Conditions	Mode of flight	Detection function availability: xPL compared to xAL	
		Actual	Assumed
Nominal Noise	APV1	1.00	-
	APV2	0.654	-
CW worst GPS line -156.5dBW	APV1	1.00	1.00
	APV2	0.577	0.654
CW worst GPS line -135.5dBW	APV1	0.828	1.00
	APV2	0.198	0.654
CW worst Galileo line -156.5dBW	APV1	1.00	1.00
	APV2	0.608	0.654
CW worst Galileo line -135.5dBW	APV1	0.835	1.00
	APV2	0.101	0.654

Tables 3 & 4- Snapshot LSR performance

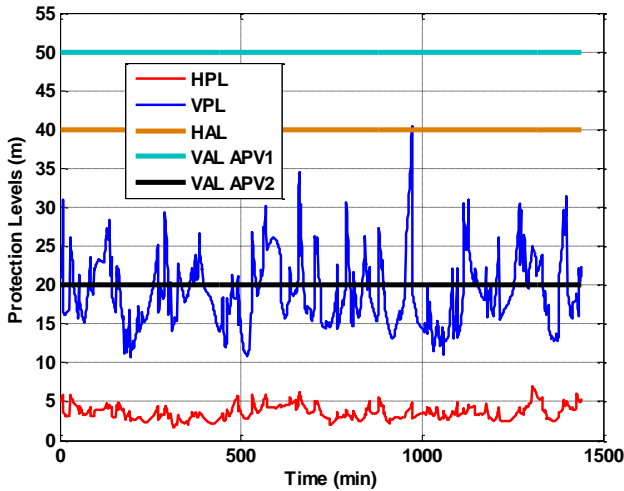


Fig 10 - RAIM LSR-APV 1 & 2 - Nominal Conditions

If a CW interference within the interference mask is present, the actual availability is 100% for APV1 operation. This is not the case for APV2 which availability depends on the chosen method.

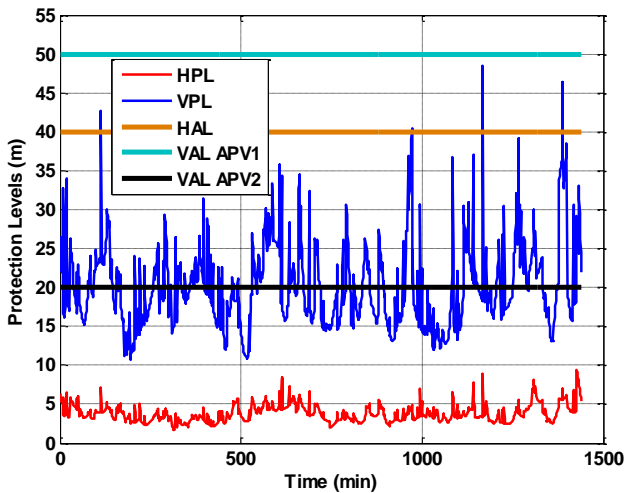


Fig 11 - RAIM LSR - APV 1 & 2 - CW on worst GPS line  $P=-156.5\text{dBW}$

Using advanced method of measuring availability, APV1 remains always available with LSR RAIM in presence of CW interference 20dB above the interference mask. This is not the case for APV2 where of detecting critical biases is seriously degraded. This situation can be hazardous for the user since he only has the xPL corresponding to nominal condition and as can be seen on fig it can lead to misleading situation (figure 13). Such situation happens 0.22% of the time if a CW interference 20dB above the mask is injected on worst GPS line.

## CONCLUSION

A complete model of pseudo range measurement has been proposed taking into account the effect of interference.

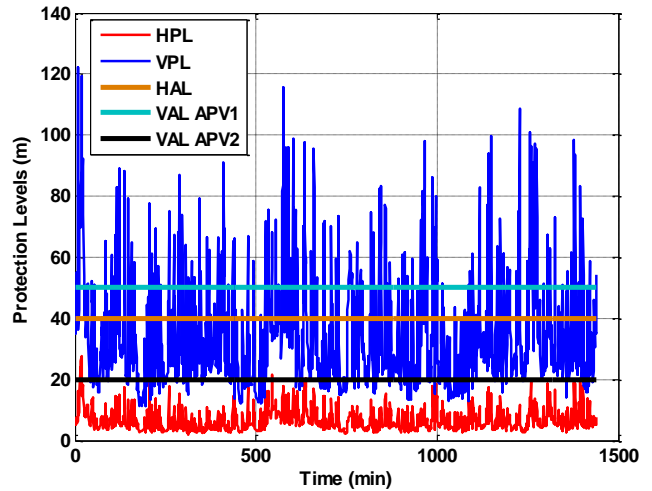


Fig 12 - RAIM LSR-APV 1 & 2 - CW on worst GPS line  $P=-135.5\text{dBW}$

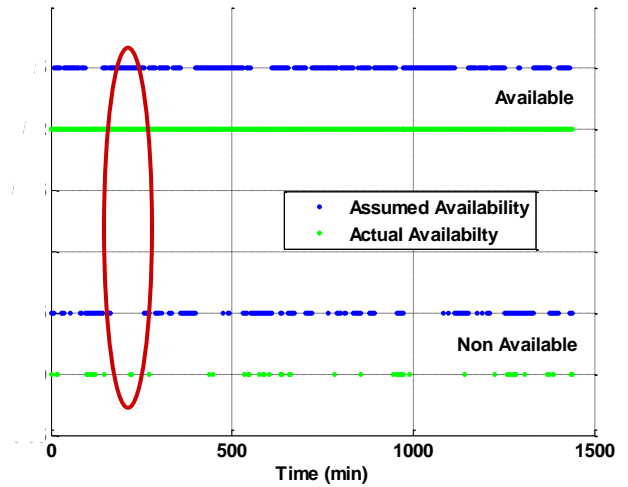


FIG 13 - RAIM LSR-APV 2 - CW on worst GPS line  $P=-135.5\text{dBW}$

Using this model, RAIM simulations has been conducted in order to analyse the impact of interference on performance.

It has been seen there is no impact of CW interference within the interference mask: Sequential GLR and Snapshot LSR RAIM performance are not degraded.

On the contrary, CW interference with a power 20 dB above the mask has an important effect on pseudo range error variance. For example, if it frequency corresponds to the worst GPS line:

- Sequential constrained GLR availability for APV2 is down from 99.9% to 98.8%
- Snapshot LSR availability for APV2 is down from 65.4% to 19.8% using actual protection levels based method of integrity monitoring

- Snapshot LSR actual availability for APV2 is down from 100% to 94.3% using critical bias detection method

In any case, if advanced methods of monitoring integrity are used (detection of critical biases), the user will be protected from hazardous misleading situation. But the actual implementation of such a RAIM remains to be done.

## APPENDIX: CRITICAL BIAS

### Definition of a positioning failure

A fault  $\gamma$  is considered as a horizontal positioning failure if its impact violates the integrity risk:

$$(1 - p_f) \max P_0 \left( \begin{array}{l} \exists t : k_0 \leq t \leq k_0 + m - 1, \\ \left\| X_{horiz,t} - \hat{X}_{horiz,t} \right\|_2 > HAL \end{array} \right) + p_f P_\gamma \left( \left\| X_{horiz,t} - \hat{X}_{horiz,t} \right\|_2 > HAL \right) > P_{IntRisk}$$

A fault  $\gamma$  is considered as a vertical positioning failure if its impact violates the integrity risk:

$$(1 - p_f) \max P_0 \left( \begin{array}{l} \exists t : k_0 \leq t \leq k_0 + m - 1, \\ \left\| X_{vertical,t} - \hat{X}_{vertical,t} \right\|_2 > VAL \end{array} \right) + p_f P_\gamma \left( \left\| X_{vertical,t} - \hat{X}_{vertical,t} \right\|_2 > VAL \right) > P_{IntRisk}$$

where  $p_f$  is the probability of failure of one satellite,  $P_0$  designed the fault free case,  $P_\gamma$  the faulty case, HAL and VAL are the horizontal and vertical alert limits

### Minimum biases that lead to a positioning failure

For each pseudorange measurement, this critical bias represents the smallest additional error that will lead to a positioning failure with a probability equal to the integrity risk.

The error in the position domain is:

$$\mathcal{E}_{pos,WGS84} = (H^T \Sigma^{-1} H)^{-1} H^T \Sigma^{-1} (\xi + B)$$

and projecting this error in the local geographic frame:

$$\mathcal{E}_{pos,local} = n_{local}^t \cdot \mathcal{E}_{pos,WGS84} \quad \text{where}$$

$$n_{local} = \begin{bmatrix} -\sin \varphi \cos \lambda & -\sin \varphi \sin \lambda & \cos \varphi & 0 \\ -\sin \lambda & \cos \lambda & 0 & 0 \\ \cos \varphi \cos \lambda & \cos \varphi \sin \lambda & \sin \varphi & 0 \\ 0 & 0 & 0 & 1 \end{bmatrix}$$

Let us define the matrix  $M = n_{local}^t \cdot (H^T \Sigma^{-1} H)^{-1} H^T \Sigma^{-1}$  in order to make the projection in the local geographic frame such as  $\mathcal{E}_{pos,local} = M(\xi + B)$

In the fault free case ( $B = 0$ ), the covariance matrix of the error such as  $\mathcal{E}_{pos,local} \sim N(0_{4 \times 1}, C)$  is :

$$C = E[\mathcal{E}_{pos,local} \cdot \mathcal{E}_{pos,local}^t] = n_{local}^t \cdot (H^T \Sigma^{-1} H)^{-1} n_{local}$$

First we look at the computation of the probability that a given error in the horizontal plane leads to a positioning failure.

If we are not in the fault free case and thus in a more general way, the horizontal positioning error is a two dimensions vector which follows a gaussian bi-dimensional law of mean impact  $\times r$  and of covariance matrix  $C_H$ . Its density function is:

$$f_0(X_H) = \frac{1}{2\pi \sqrt{\det C_H}} \exp\left(-\frac{1}{2} X_H^t C_H^{-1} X_H\right)$$

Considering this in the space of singular values decomposition of  $C_H$  and denoting  $\lambda_1$  and  $\lambda_2$  the two eigenvalues of this covariance matrix:

$$f_0(X_{H\perp}) = \frac{1}{2\pi \sqrt{\lambda_1 \lambda_2}} \exp\left(-\frac{1}{2} \left( \frac{(x - \Omega_1)^2}{\lambda_1} + \frac{(y - \Omega_2)^2}{\lambda_2} \right)\right)$$

where  $X_{H\perp} = \begin{bmatrix} x \\ y \end{bmatrix}$  and  $\begin{bmatrix} \Omega_1 \\ \Omega_2 \end{bmatrix}$  is due to the change of coordinates.

The probability that a couple  $(x, y)$  be such that  $x^2 + y^2 \leq HAL^2$  considering its distribution is:

$$P(X_H \in D) = \iint_D \frac{1}{2\pi \sqrt{\lambda_1 \lambda_2}} \exp\left(-\frac{1}{2} \left( \frac{(x - \Omega_1)^2}{\lambda_1} + \frac{(y - \Omega_2)^2}{\lambda_2} \right)\right) dx dy$$

denoting D the domain such as  $x^2 + y^2 \leq HAL^2$ .

Let's make a change of coordinates such as we could have  $\frac{(x - \Omega_1)^2}{\lambda_1} + \frac{(y - \Omega_2)^2}{\lambda_2} = r^2$ . We re-write  $(x, y)$  this way:

$$\begin{cases} x = \Omega_1 + r \sqrt{\lambda_1} \cos \theta \\ y = \Omega_2 + r \sqrt{\lambda_2} \sin \theta \end{cases}$$

The equation  $x^2 + y^2 = HAL^2$  that defines the boundaries of the integration domain becomes:

$$\begin{aligned} x^2 + y^2 &= (\Omega_1 + r \sqrt{\lambda_1} \cos \theta)^2 + (\Omega_2 + r \sqrt{\lambda_2} \sin \theta)^2 \\ &= \Omega_1^2 + r^2 \lambda_1 \cos^2 \theta + 2\Omega_1 r \lambda_1 \cos \theta \\ &\quad + \Omega_2^2 + r^2 \lambda_2 \sin^2 \theta + 2\Omega_2 r \lambda_2 \sin \theta = HAL^2 \end{aligned}$$

Solving this equation, two roots  $r_1(\theta)$  and  $r_2(\theta)$  for  $\theta \in [0, \pi]$  are obtained such as:

$$\begin{cases} x = \Omega_1 + r_1(\theta)\sqrt{\lambda_1} \cos \theta \\ y = \Omega_2 + r_1(\theta)\sqrt{\lambda_2} \sin \theta \end{cases}, \theta \in [0, \pi] \quad \text{and}$$

$$\begin{cases} x = \Omega_1 + r_2(\theta)\sqrt{\lambda_1} \cos \theta \\ y = \Omega_2 + r_2(\theta)\sqrt{\lambda_2} \sin \theta \end{cases}, \theta \in [0, \pi] \quad \text{define the}$$

boundaries of the integration domain.

The jacobian of this transformation is computed to make our change of coordinates  $J = |r|\sqrt{\lambda_1\lambda_2}$ , and:

$$P(X_H \in D) = \iint_{D'} \frac{|r|}{2\pi} \exp\left(-r^2/2\right) dr d\theta$$

where the new domain  $D'$  is defined by

$$\begin{cases} (r - r_1(\theta))(r - r_2(\theta)) \leq 0 \\ \theta \in [0, \pi] \end{cases}$$

Considering properties of second order polynomials:

$$P(X_H \in D) = \frac{1}{2\pi} \int_{\theta=0}^{\theta=\pi} \int_{r=r_1(\theta)}^{r=r_2(\theta)} |r| \exp\left(-r^2/2\right) dr d\theta$$

Assuming for example that  $r_1 \leq 0 \leq r_2$ ,

$$P(X_H \in D) = \frac{1}{2\pi} \times \int_{\theta=0}^{\theta=\pi} \left[ - \int_{r=r_2}^{r=0} r \exp\left(-r^2/2\right) dz + \int_{r=0}^{r=r_1} r \exp\left(-r^2/2\right) dr \right] d\theta$$

$$P(X_H \in D) = 1 - \frac{1}{2\pi} \int_{\theta=0}^{\theta=\pi} \left[ \exp\left(-r_2^2/2\right) + \exp\left(-r_1^2/2\right) \right] d\theta$$

and this last integral is computed numerically.

Thus the probability that the point  $(x, y)$  is out of the circle of radius  $HAL$  is:

$$P(X_H \notin D) = \frac{1}{2\pi} \int_{\theta=0}^{\theta=\pi} \left[ \exp\left(-r_2^2/2\right) + \exp\left(-r_1^2/2\right) \right] d\theta$$

In order to pass from a bias  $b$  on a given pseudo range to an error vector in the local horizontal plane, projections are made using linear relations. Denoting

$A = (H^T H)^{-1} H^T$  we define for  $i \in [1, N]$ :

$$H_{pseudo\_pos\_North}(i) = |A_{1,i}|$$

and  $H_{pseudo\_pos\_East}(i) = |A_{2,i}|$

An equivalent analysis of the vertical risk (which is easier in one dimension) must also be done. Then by comparing successively the obtained probabilities with the integrity risk for different bias amplitudes, the minimum bias

which leads to a positioning failure with a probability equal to the integrity risk is finally obtained.

## REFERENCES

- [1] Nikiforov, I., B. Roturier (2005) Convention STNA - Astrée, Final report Autonomous integrity monitoring of the GNSS
- [2] RTCA/ DO 229C (2001), "Minimum Operational Performance Standards for Global Positioning Systems / Wide Area Augmentation System Airborne Equipment", RTCA, Inc., Washington D.C., USA.
- [3] Macabiau, C., A. Martineau, O. Julien (2007), "Model of Pseudorange Measurement Error due to Interference", ENAC internal report.
- [4] Betz J. (2000), "Effect of Narrowband Interference on GPS Code Tracking Accuracy", ION NTM 2000.
- [5] Betz J., K. Kolodziejski (2001), "Extended Theory of Early-Late Code-Tracking for a Band limited GPS Receiver", Mitre Report.
- [6] Macabiau C., L. Moriella, M. Raimondi, C. Dupouy, A. Steingass, A. Lehner (2006), "GNSS Airborne Multipath Errors Distribution Using the High Resolution Aeronautical Channel Model and Comparison to SARPs Error Curve", ION NTM 2006, January.
- [7] EUROCAE WG 62, "Interim Minimum Operational Performance Specification for Airborne Galileo Satellite Receiver Equipment", White paper, may 2006.
- [8] Clot A., C. Macabiau, I. Nikiforov, B. Roturier (2006), "Sequential RAIM designed to detect Combined Step Ramp Pseudo-Range Errors" ION GNSS 2006.
- [9] Hegarty C. (1996), "Analytical Derivation of Maximum Tolerable In-Band Interference Level for Aviation Applications of GNSS"
- [10] Julien O. (2005), "Design of Galileo L1F tracking loops", Ph.D. thesis, University of Calgary, Department of Geomatics Engineering
- [11] Julien O., C. Macabiau (2006), "What are the major differences between Galileo and GPS current and forthcoming frequencies?", GNSS Solutions column, Inside GNSS, Vol. 1, Number 3, 2006.
- [12] Rebeyrol E., C. Macabiau (2005), "BOC power spectrum densities", ION NTM 2005, January.